

Weak-boson production at Fermilab Tevatron energies

E. L. Berger

High Energy Physics Division, Argonne National Laboratory, Argonne, Illinois 60439

F. Halzen, C. S. Kim, and S. Willenbrock

Department of Physics, University of Wisconsin, Madison, Wisconsin 53706

(Received 19 May 1988)

Weak bosons are produced in hadron collisions by quarks and antiquarks with average fractional momenta $x = M_{W,Z}/\sqrt{s}$. When \sqrt{s} is increased by a factor of 3, the average value of x shifts from about 0.15 at CERN $p\bar{p}$ collider energies to 0.05 at the Fermilab Tevatron, i.e., from a regime where valence quarks dominate to a regime where sea quarks dominate the production features of weak bosons. We investigate systematically the problem of calculating W and Z cross sections in this new regime, paying special attention to the ratio $\sigma(W)/\sigma(Z)$ which is necessary for determining the ratio of total widths $\Gamma(W)/\Gamma(Z)$ from hadron-collider data. We emphasize that with the increased statistics in $p\bar{p}$ experiments, the parton fluxes responsible for the production of weak bosons can be controlled internally by a study of the asymmetry of the rapidity distribution of the W boson. We derive a relation between the asymmetry in W^\pm rapidity distributions and the ratio F_2^n/F_2^p of deep-inelastic lepton-hadron scattering structure functions. The production rates of weak bosons also become sensitive to production via the charm quark. This calculation raises some interesting theoretical issues. We discuss both problems in detail. We also study the implications of our results for the determination of the number of light neutrinos and the mass of the top quark via a measurement of the W -to- Z event ratio.

I. INTRODUCTION

Measurement of the W and Z production cross sections and momentum distributions in $p\bar{p}$ interactions at the increased energy of the Fermilab collider ($\sqrt{s} = 1.8$ TeV) will test the standard model in a new kinematic regime. The electroweak sector of the standard model is tested in principle by measurement of the W and Z widths. As this is difficult in practice, one concentrates instead on the measurement of the ratio of branching ratios $B(W \rightarrow e\nu)/B(Z \rightarrow e^+e^-)$ which is determined from the relative frequency of W and Z events $\sigma(p\bar{p} \rightarrow W \rightarrow e\nu)/\sigma(p\bar{p} \rightarrow Z \rightarrow e^+e^-)$ and the calculated cross-section ratio $\sigma(p\bar{p} \rightarrow W)/\sigma(p\bar{p} \rightarrow Z) \equiv \sigma(W)/\sigma(Z)$. The ratio $B(W \rightarrow e\nu)/B(Z \rightarrow e^+e^-)$ is predicted¹ by the standard model in terms of three parameters: the Weinberg angle θ_W , the number of light neutrino flavors N_ν , and the mass m_t of the top quark. Physics beyond the standard model, i.e., new decays of the W and Z or mixing of the Z with heavier Z 's will modify its value.² Thus, a detailed scrutiny of $B(W \rightarrow e\nu)/B(Z \rightarrow e^+e^-)$ should be a high priority. This test of the electroweak model is limited by the precision with which we can calculate $\sigma(W)/\sigma(Z)$. This is a new and systematically different problem at Fermilab Tevatron energies.

The problem has two novel aspects resulting from increased collision energies. As the average fractional momentum of a parton producing a W (or Z) is $x = M_{W,Z}/\sqrt{s} \simeq 0.05$, we move into a regime where sea quarks are the dominant source of weak bosons. Not only the ratio of valence u - and d -quark distributions, but also the structure of the sea affects our understanding of $\sigma(W)/\sigma(Z)$; see Fig. 1. We emphasize how measure-

ments of W and Z rapidity distributions in collider experiments can be exploited to determine the parton fluxes which are responsible for weak-boson production, reducing reliance on parton densities fitted to data encompassing lower- Q^2 values from experiments with very different systematic uncertainties.

The presence of charm inside the colliding p and \bar{p} is responsible for weak-boson production via $c\bar{s} \rightarrow W$ and $c\bar{c} \rightarrow Z$. This contribution becomes relevant at Tevatron energies and is increasingly important for higher-energy collisions. The cross section $c\bar{s} \rightarrow W$ is ~ 1 nb at $\sqrt{s} = 1.8$ TeV and is therefore observable directly with the 1 pb^{-1} expected luminosity. It gives us a new probe of the charm content of the proton.

Although $\sigma(W)/\sigma(Z)$ is determined to high precision at the quark level, the parton flux factor $(u\bar{d} + \bar{u}d)/(u\bar{u} + d\bar{d})$ introduces a major source of uncertainty. The flux factor enters into the calculation because the u - and d -quark distributions are not identical. It is well known that this difference is determined by the ratio of n, p deep-inelastic structure functions F_2^n/F_2^p . Following this logic^{3,4} one can extract $\sigma(W)/\sigma(Z)$ directly from two recent high-statistics CERN experiments^{5,6} by the Bologna-CERN-Dubna-Munich-Saclay (BCDMS) Collaboration and the European Muon Collaboration (EMC). We obtain, for $\sqrt{s} = 630$ GeV,

$$\frac{\sigma(W)}{\sigma(Z)} \equiv \frac{\sigma(p\bar{p} \rightarrow W^\pm)}{\sigma(p\bar{p} \rightarrow Z)} \simeq \begin{cases} 3.33 \pm 0.03 & (\text{BCDMS}), \\ 3.41 \pm 0.04 & (\text{EMC}). \end{cases} \quad (1)$$

We return however empty handed as the two results disagree by more than 2σ , reflecting inconsistent input data on F_2^n/F_2^p , as shown in Fig. 2.

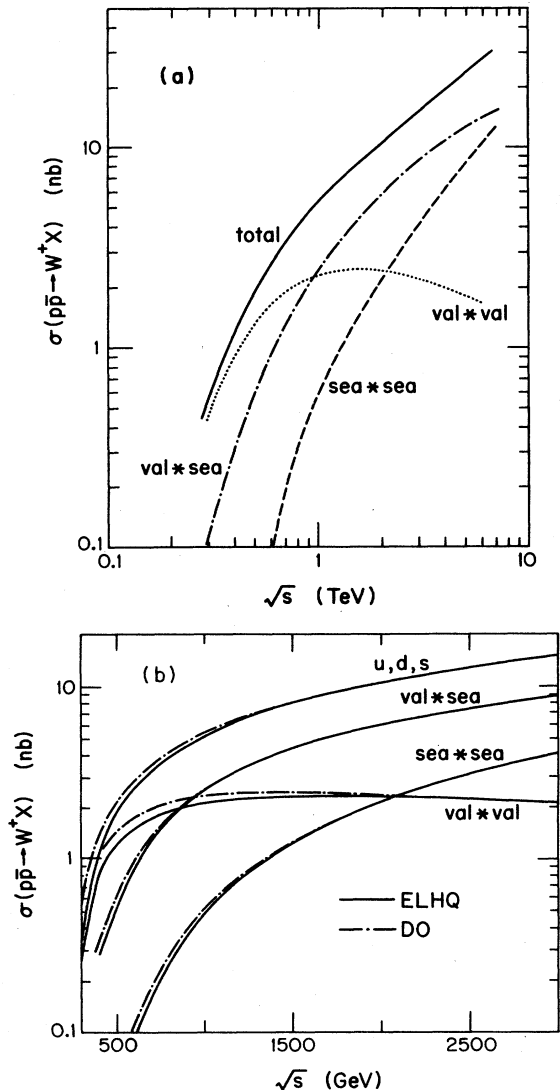


FIG. 1. W production cross section in $p\bar{p}$ collisions as a function of \sqrt{s} . Also shown are the separate contributions from valence-valence, valence-sea, and sea-sea quark interactions. The parton densities of (a) MRS 1, and (b) EHLQ 1 and DO 1 were used.

One possible way out of this dilemma is by brute force.⁷ One repeats the calculation for all previous measurements of F_2^n/F_2^p and subsequently averages all (seven) results. This procedure yields a value $\sigma(W)/\sigma(Z) = 3.39 \pm 0.05$ favoring the EMC result, at least at $x = m_W/\sqrt{s}$. This approach has the advantage that experiments with very different systematic errors are averaged. The disadvantage is that some data are from a kinematic regime where $Q^2 \ll m_W^2$. This drawback is in principle not a problem as the Q^2 dependence is calculable and very weak.

In this paper we describe how collider data can resolve the present impasse without reliance on deep-inelastic lepton scattering data, especially those corresponding to small Q^2 values. We show how measurement of the asymmetry of the rapidity distribution of W^\pm production

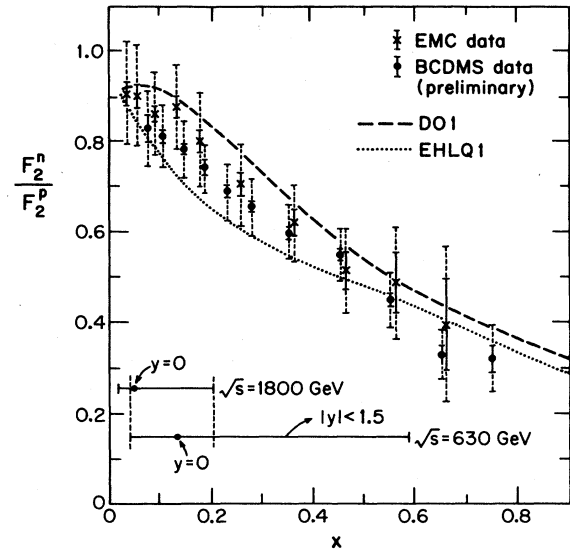


FIG. 2. Data on F_2^n/F_2^p of BCDMS (Ref. 6) and EMC (Ref. 5) are compared with calculations based on EHLQ 1 and DO 1 parton densities, adapted from Colas, Denegri, and Stubenrauch (Ref. 4). Also shown is the explorable range of proton momentum fraction x at $\sqrt{s} = 630$ GeV and 1.8 TeV if the W -boson cross section is measured over the rapidity region of $|y| < 1.5$.

in $p\bar{p}$ collisions allows for a sufficiently precise determination of the u/d ratio so that Γ_W/Γ_Z can be determined to good precision. This measurement can resolve the BCDMS-EMC disagreement of Eq. (1) after about 2000 reconstructed W^\pm events are accumulated. This is within easy range of both the upgraded CERN $p\bar{p}$ collider (ACOL) and the Tevatron. In independent measurements the u - and d -quark distributions will be extracted over a range of x values including the value $x = m_W/\sqrt{s}$ relevant for the determination of Γ_W/Γ_Z . The collider experiments can eventually match the statistics of deep-inelastic scattering experiments and permit a determination of parton densities not plagued by conflicting lepton scattering data.

The outline of the paper is as follows. In Sec. II we discuss in detail how rapidity measurements of weak bosons can be used to improve the experimental determination of $u(x)/d(x)$ and of $\sigma(W)/\sigma(Z)$. In Sec. III we predict $\sigma(W)/\sigma(Z)$ at $\sqrt{s} = 1.8$ TeV to be about 3.1 without inclusion of charm-quark contributions, and we estimate the various sources of error. The prediction is raised to about 3.24 when the charm-quark contributions are included. Further experiments will translate these results into limits on the number of light neutrinos and possibly the top mass. In Sec. IV we discuss the associated production of W , Z , and charm emphasizing that this process [detected, e.g., as $W(\rightarrow l)c(\rightarrow \bar{l})$ dilepton final states] can provide us with a first direct measurement of the charm content of the nucleon.

II. ASYMMETRY IN THE RAPIDITY DISTRIBUTION

In calculations of $R_\sigma \equiv \sigma(W)/\sigma(Z)$, a significant source of uncertainty is simply that different choices of

parton densities give different results. This uncertainty is to a large extent associated with different parametrizations of the ratio of the valence up-quark to the valence down-quark densities in a proton. To reduce this uncertainty, several authors^{3,4} have explored the direct use of data on the ratio $F_2^n(x, Q^2)/F_2^p(x, Q^2)$, measured in deep-inelastic lepton scattering, to constrain calculations of R_σ . Doing so, one may conclude that the estimated uncertainty in R_σ at CERN collider energies is significantly smaller than that obtained from comparing results obtained from different choices of parton densities.

While certainly an improvement, methods based on use of the data on $F_2^n(x, Q^2)/F_2^p(x, Q^2)$ have their own limitations. First, the deep-inelastic data, however accurate, do not cover the regions of small x probed at Fermilab Tevatron energies ($0.016 < x < 0.12$) for W production in

the interval $-1 < y < 1$. Second, the sensitivity of the deep-inelastic ratio to the required $u_V(x)/d_V(x)$ diminishes as x decreases. Third, the structure functions are required at a scale $Q^2 = M_{W,Z}^2$, well above the values examined in deep-inelastic scattering. Although the change with Q^2 of the ratio $F_2^n(x, Q^2)/F_2^p(x, Q^2)$ is predicted to be small in leading-order QCD, there is hidden uncertainty associated with potential higher-twist components in the deep-inelastic data at low Q^2 . Finally, deep-inelastic data on $F_2^n(x, Q^2)/F_2^p(x, Q^2)$ require comparison of results from different targets, implying the presence of systematic uncertainties in the experimental ratio itself.

In the method which we shall now describe all of the above sources of uncertainty are eliminated, leaving only statistical precision as the controlling limitation.

The inclusive rapidity distribution for production of a W^+ boson in $p\bar{p}$ collisions is expressed as

$$\frac{d\sigma}{dy}(p\bar{p} \rightarrow W^+ X) = K(y) \frac{2\pi G_F}{3\sqrt{2}} x_1 x_2 \{ \cos^2\theta_C [u(x_1)d(x_2) + \bar{d}(x_1)\bar{u}(x_2)] + \sin^2\theta_C [u(x_1)s(x_2) + \bar{s}(x_1)\bar{u}(x_2)] \}, \quad (2)$$

$$x_1 = \frac{M_W}{\sqrt{s}} \exp(y), \quad x_2 = \frac{M_W}{\sqrt{s}} e^{-y}.$$

In this expression, contributions from the charm quark and heavier flavors are ignored; we will discuss them below. All quark (u, d, s) and antiquark ($\bar{u}, \bar{d}, \bar{s}$) densities are those of a proton. Dependences on Q^2 have been suppressed, but it is understood that, e.g., $u(x) \equiv u(x, M_W^2)$. The factor $K(y)$ is associated with higher-order contributions⁸ in QCD. The rapidity distributions $d\sigma(W^+)/dy$ and $[d\sigma(W^+)/dy]/[d\sigma(Z)/dy]$ are shown in Fig. 3.

The factor $K(y)$ is calculated⁸ from

$$K(y) = [\sigma_{DY}(y) + \sigma_R(y) + \sigma_V(y) + \sigma_{CS}(y)] / \sigma_{DY}(y), \quad (3)$$

where σ_{DY} is the cross section for the lowest-order Drell-Yan process $q\bar{q} \rightarrow W$, σ_R the σ_{DY} with radiation of a real gluon, σ_V the σ_{DY} with vertex correction, and σ_{CS} the Compton scattering (i.e., $qg \rightarrow q'W$).

The asymmetry in the rapidity distribution is defined as

$$A_{W^+}(\sqrt{s}, y) = A_{W^-}(\sqrt{s}, -y) = \frac{\sigma_{W^+}(\sqrt{s}, y) - \sigma_{W^+}(\sqrt{s}, -y)}{\sigma_{W^+}(\sqrt{s}, y) + \sigma_{W^+}(\sqrt{s}, -y)}. \quad (4)$$

Making the assumption of an SU(2)-symmetric sea [$\bar{u}(x) = \bar{d}(x)$], and dropping terms (see below) which are very small numerically, we derive the expressions

$$A(y) \simeq \frac{1}{D(\sqrt{s}, y)} \left[\frac{u(x_1) - d(x_1)}{u(x_1) + d(x_1)} - \frac{u(x_2) - d(x_2)}{u(x_2) + d(x_2)} \right] + \frac{K(y) - K(-y)}{K(y) + K(-y)}. \quad (5)$$

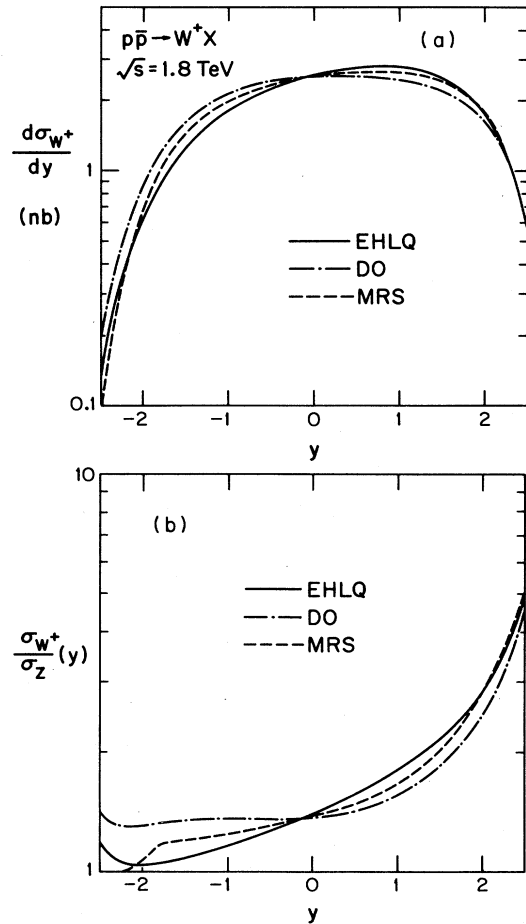


FIG. 3. Rapidity distribution ($-2.5 \leq y \leq 2.5$) of (a) W^+ production, and (b) the W^+ -to- Z production ratio $(d\sigma_{W^+}/dy)/(d\sigma_Z/dy)$ at the Tevatron ($\sqrt{s} = 1.8$ TeV) based on the parton densities of EHLQ 1, DO 1, and MRS 1.

Here

$$D(\sqrt{s}, y) = 1 - \frac{u(x_1) - d(x_1)}{u(x_1) + d(x_1)} \frac{u(x_2) - d(x_2)}{u(x_2) + d(x_2)} + \frac{\bar{u}(x_1) + \bar{d}(x_1)}{u(x_1) + d(x_1)} \frac{\bar{u}(x_2) + \bar{d}(x_2)}{u(x_2) + d(x_2)}. \quad (6)$$

Terms proportional to $\tan^2 \theta_c \simeq 0.05$ are very small numerically and have been dropped from the expressions for $A(y)$ and $D(\sqrt{s}, y)$. Also omitted from these analytic expressions are negligible next-order terms that are proportional to the product of two small quantities

$$[K(y) - K(-y)][u(x_1) - d(x_1) - u(x_2) + d(x_2)].$$

In the full expression for $d\sigma/dy$, there are terms proportional to $[c(x_1)s(x_2) + \bar{s}(x_1)\bar{c}(x_2)]$, to be discussed in Sec. IV. However, these cancel in $A(y)$ because $c(x_1) = \bar{c}(x_1)$ and $s(x_1) = \bar{s}(x_1)$. Moreover, the other contributions to $A(y)$ from c - and s -quark densities ($\propto us$ and cd) tend to cancel, resulting in a combined contribution to $A(y)$ for $|y| < 1.5$ of less than 0.6% at $\sqrt{s} = 630$ GeV and 0.2% at $\sqrt{s} = 1.8$ TeV.

In the region of small x_1 and x_2 of interest at Tevatron energies, and with the rapidity in the range $-1 < y < 1$, the symmetric function $D(\sqrt{s}, y)$ is fairly constant, with $D(\sqrt{s}, y) \simeq 1.1$. Furthermore, $D \rightarrow 1$ as y approaches its maximum allowed value.

Higher-order corrections do not contribute significantly to the asymmetry. After explicit numerical evaluation, we find $K(-y)/K(y) = 1$ ($y=0$), 0.99 ($y < 0.5$), and 0.97 ($y < 1.5$).

From Eq. (5), we conclude that the asymmetry $A(y)$ provides an excellent determination of the ratio $u(x, Q^2)/d(x, Q^2)$ in the region of x and Q^2 where it is most relevant for specification of R_σ . Using the linear approximation $d(x)/u(x) = 1 - ax$ appropriate for the limited range of x of interest to us, we derive

$$A(y) \simeq a \frac{M_W}{\sqrt{s}} \sinh y. \quad (7)$$

A measurement of $A(y)$ therefore determines the effective slope a . (To avoid misunderstanding, we note that the slope a is a function of M_W/\sqrt{s} . This should be kept in mind if results at CERN and Fermilab energies are compared. Since the typical value of x changes from $x \simeq 0.130$ to 0.045 for W production at $\sqrt{s} = 630$ GeV and $\sqrt{s} = 1.8$ TeV, respectively, the point at which one determines the slope a changes.)

In Fig. 4 we show predictions of $A(y)$ obtained from three sets of parton densities.⁹⁻¹¹ The x dependence of the ratio $d(x, Q^2)/u(x, Q^2)$ for the same three sets of parton densities is shown in Fig. 5. Comparison of Figs. 4 and 5 shows that the slope in y of $A(y)$ near $y=0$ reflects directly the slope in x of $d(x, Q^2)/u(x, Q^2)$ in the region of x of interest at the Tevatron collider.

At the present time, the curves in Fig. 4 can be taken as predictions. The differences among the curves may be used to estimate the experimental statistical precision needed to pin down the appropriate parametrization of

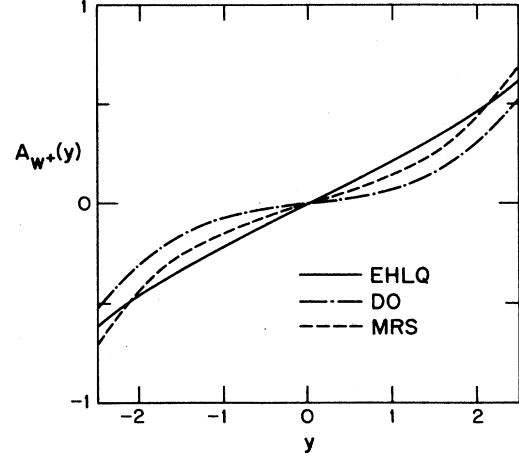


FIG. 4. Asymmetry $A(y)$ of the rapidity distribution for W^+ production at the Tevatron.

$u(x)/d(x)$ at collider energies.¹² Roughly 2000 reconstructed $W^\pm \rightarrow e\nu$ are expected at $\sqrt{s} = 1.8$ TeV in the Collider Detector at Fermilab (CDF) for an integrated luminosity of 2 pb^{-1} . At $\sqrt{s} = 1.8$ TeV, the predicted $A(y)$ at $y=1$ ranges from $A(y=1) = 0.07$ (DO 1) to 0.21 (EHLQ 1), whereas at $\sqrt{s} = 0.63$ TeV, the values are $A(y=1) = 0.27$ (DO 1) to 0.42 (EHLQ 1). With 2000 reconstructed W^\pm spread over 10 bins in $|y|$, $|y|=0$ to 2, the statistical uncertainty *per bin* is 7%, comparable to the smaller value of $A(y=1)$ expected theoretically at $\sqrt{s} = 1.8$ TeV. The asymmetry measurements we envisage appear quite feasible.

Once good data are available on $A(y)$, the data themselves can be used to fix $d(x, M_W^2)/u(x, M_W^2)$ which, in turn, will permit precise calculations of R_σ . This is especially valuable since it permits an analysis of Tevatron data on R_σ constrained by data on $d(x, Q^2)/u(x, Q^2)$ obtained from the same experiment in the relevant regions of x and Q^2 . Correspondingly, theoretical uncertainties will be significantly reduced in attempts to determine

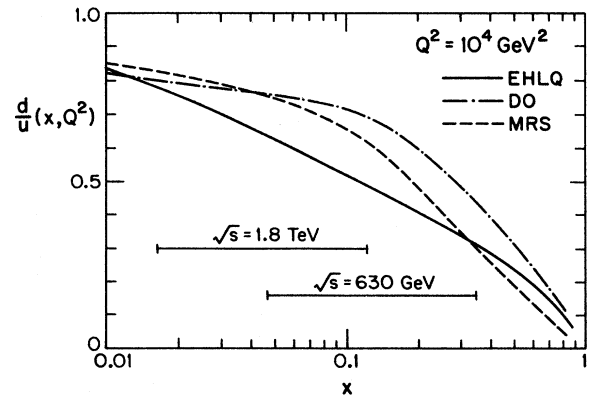


FIG. 5. The ratio $d(x, Q^2)/u(x, Q^2)$ at $Q^2 = 10^4 \text{ GeV}^2$ and $0.01 < x < 1.0$, which is directly related to $A(y)$ in Fig. 4.

upper limits on N_ν and m_t .

In order to resolve the problem of the ratio F_2^n/F_2^p (i.e., BCDMS vs EMC), we express the ratio F_2^n/F_2^p as

$$\begin{aligned} \frac{F_2^n}{F_2^p}(x, Q^2=Q_{\text{DIS}}^2) &\simeq \frac{F_2^n}{F_2^p}(x, Q^2=M_W^2) \\ &= \frac{u+4d+7S}{4u+d+7S}, \end{aligned} \quad (8)$$

assuming an SU(3)-symmetric sea, i.e., $\bar{u}=\bar{d}=s=\bar{s}=S$. [For an SU(2)-symmetric sea, i.e., $\bar{u}=\bar{d}=\bar{S}$, replace $7S$ by $5\bar{S}+2s$.] $Q_{\text{DIS}}^2 \simeq (10 \text{ GeV})^2$ is the average Q^2 value for the CERN muon measurements of F_2^n/F_2^p . The combination of Eqs. (5) and (8) yields the relation

$$A_{W^+}(\sqrt{s}, y) \simeq \frac{1}{D(\sqrt{s}, y)} \sum_{i=1}^2 (-1)^{i+1} T(x_i) \left[1 - \frac{F_2^n}{F_2^p}(x_i) \right] \quad (9)$$

with

$$T(x_i) = \frac{1}{3} \left[4 - \frac{3d_i - 7S_i}{u_i + d_i} \right]. \quad (10)$$

Equation (9) relates directly the two measurements A and F_2^n/F_2^p . The functions D and T turn out to be fairly constant and well determined by standard parton density analyses. The numerical value of $T(x_i)/D(\sqrt{s}, y)$ is almost independent of \sqrt{s}, y and of the parton densities. It is numerically about 1.2 for $|y| < 1$. Therefore Eq. (9) can be approximated as

$$A_{W^+}(\sqrt{s}, y) \simeq 1.2 \left[\frac{F_2^n}{F_2^p}(x_2) - \frac{F_2^n}{F_2^p}(x_1) \right]. \quad (11)$$

Equation (11) enables us to determine the slope of the ratio F_2^n/F_2^p directly. This is an important alternative method to study the difference between the u - d -quark structure of the nucleon. It is not affected by ambiguities related to higher-twist and nuclear target effects.

Straightforward use of statistics shows that to measure F_2^n/F_2^p to better than 3%, the required precision to differentiate between the two sets of data in Fig. 2, it is necessary to measure the asymmetry to better than 4%. About 2000 reconstructed W^\pm events are required. In a final analysis, uncertainties associated with the functions D, T and higher-order contributions must be taken in to account. We estimate these errors to be less than 6% (2%) at ACOL (Tevatron). The asymmetry A varies with \sqrt{s} , whereas the ratio F_2^n/F_2^p does not. This energy dependence allows for two separate measurements at CERN and Fermilab, covering independently the region $0.03 < x < 0.2$ which is crucial for the determination of $\sigma(W)/\sigma(Z)$.

III. $B(W \rightarrow e\nu)/B(Z \rightarrow e^+e^-)$

AND A LIMIT ON THE NUMBER OF NEUTRINOS

Within the standard model with three generations, the experimentally observed ratio R of $W \rightarrow e\nu$ and $Z \rightarrow e^+e^-$ events in $p\bar{p}$ colliders allows for a high-

precision test of the standard electroweak theory. A measurement of R is equivalent¹ to an experimental determination of $\Gamma(W)/\Gamma(Z)$ and therefore a measurement of (or limit on) the mass of the top quark, which is the only remaining parameter in the standard-model value of $\Gamma(W)/\Gamma(Z)$. Alternatively, given the top-quark mass, the ratio determines the number of light neutrino flavors, as any neutrino beyond $N_\nu=3$ adds 167 ± 9 MeV to $\Gamma(Z)$ and thus modifies the detailed balance present in the measured ratio.

The procedure exploits the identity

$$\begin{aligned} R &\equiv \frac{\sigma(p\bar{p} \rightarrow W \rightarrow e\nu)}{\sigma(p\bar{p} \rightarrow Z \rightarrow e^+e^-)} \\ &= \left[\frac{\Gamma(W \rightarrow e\nu)/\Gamma(W)}{\Gamma(Z \rightarrow e^+e^-)/\Gamma(Z)} \right] \frac{\sigma(W)}{\sigma(Z)} = R_\Gamma R_\sigma. \end{aligned} \quad (12)$$

The ratio of branching ratios R_Γ is determined by standard electroweak couplings¹³

$$\begin{aligned} \Gamma(Z) &= [N_\nu + 3F_l + 3F_d + (2F_u + F_t)]\Gamma(Z \rightarrow \nu\bar{\nu}), \\ \Gamma(W) &= [3 + (2H_u + H_t)]\Gamma(W \rightarrow e\nu). \end{aligned} \quad (13)$$

Here N_ν is the number of light neutrino flavors, and subscripts l, d, u, t , respectively, denote the contributions from a charged lepton, a charge $-\frac{1}{3}$ down-type quark, a charge $+\frac{2}{3}$ up-type quark, and the top quark. In Eq. (13),

$$\begin{aligned} F_l &= 8(g_V^2 + g_A^2) \simeq 0.5, \\ F_d &= 24(g_V^2 + g_A^2) \left[1 + \frac{\alpha_s}{\pi} \right] \simeq 2.3, \\ F_u &= 24(g_V^2 + g_A^2) \left[1 + \frac{\alpha_s}{\pi} \right] \simeq 1.8, \\ F_t &= 24\beta_t [c_V^2(1 + 2m_t^2/M_Z^2) + c_A^2(1 - 4m_t^2/M_Z^2)], \\ H_u &= 3 \left[1 + \frac{\alpha_s}{\pi} \right] \simeq 3.1, \\ H_t &= 3 \left[1 + \frac{\alpha_s}{\pi} \right] \left[1 - \frac{3}{2}(m_t^2/M_W^2) + \frac{1}{2}(m_t^2/M_W^2)^3 \right], \end{aligned} \quad (14)$$

where

$$\begin{aligned} g_V &= \frac{1}{2}T_3 - Q \sin^2\theta_W, \\ g_A &= -\frac{1}{2}T_3, \\ c_V &= g_V \left\{ 1 + \frac{4\alpha_s}{3} \left[\frac{\pi}{2\beta_t} - \frac{3+\beta_t}{4} \left[\frac{\pi}{2} - \frac{3}{4\pi} \right] \right] \right\}^{1/2}, \\ c_A &= g_A \left\{ 1 + \frac{4\alpha_s}{3} \left[\frac{\pi}{2\beta_t} - \left[\frac{19}{10} - \frac{22}{5}\beta_t + \frac{7}{2}\beta_t^2 \right] \right. \right. \\ &\quad \left. \left. \times \left[\frac{\pi}{2} - \frac{3}{4\pi} \right] \right] \right\}^{1/2}, \end{aligned} \quad (15)$$

$$\beta_t = (1 - 4m_t^2/M_Z^2)^{1/2}.$$

Thus the ratio of branching ratios R_Γ may be expressed as

$$R_\Gamma = \frac{N_\nu + 3F_l + 3F_d + (2F_u + F_t)}{(3 + 2H_u + H_t)F_l}. \quad (16)$$

The ratio of W to Z cross sections, R_σ , is one of the most reliable predictions of QCD, as every diagram producing a W also produces a Z , up to $O(\alpha_s^2)$ where additional diagrams produce Z via a triangular quark loop.¹⁴ Even this contribution would vanish for equal-mass up- and down-type quarks. Therefore

$$\frac{\sigma(q\bar{q}' \rightarrow W)}{\sigma(q\bar{q} \rightarrow Z)} = (\text{ratios of known couplings}) + O(\alpha_s^2) \left[\frac{m_t^2 - m_b^2}{M_Z^2} \right]. \quad (17)$$

These $O(\alpha_s^2)$ contributions have been calculated,¹⁵ and are less than 1%, even for a very heavy top quark. We shall ignore them henceforth.

The biggest uncertainty in R_σ resides in the parton flux factors relating $q\bar{q}$ and $p\bar{p}$ cross sections, as discussed in Sec. II. The ratio of flux factors is of the form $(u\bar{d} + \bar{u}d)/(u\bar{u} + d\bar{d} + s\bar{s})$, and therefore depends on the relative fluxes of u , d , and s rather than on u , d , and s individually. The BCDMS (Ref. 6) and EMC (Ref. 5) experiments have recently extracted F_2^n/F_2^p with increased precision from deep-inelastic muon scattering. We can use these data to extract the relation between u , d , and s , via

$$\frac{F_2^n}{F_2^p} = \frac{u_V + 4d_V + (10\bar{S} + 2s)}{4u_V + d_V + (10\bar{S} + 2s)} \quad (18)$$

assuming an SU(2)-symmetric sea, i.e., $\bar{u} = \bar{d} \equiv \bar{S}$ [e.g., EHLQ, GHR (Ref. 16)] and

$$\frac{F_2^n}{F_2^p} = \frac{u_V + 4d_V + 12\bar{S}}{4u_V + d_V + 12\bar{S}} \quad (19)$$

assuming an SU(3)-symmetric sea, i.e., $\bar{u} = \bar{d} = s = \bar{s} \equiv S$ [e.g., DO, OR (Ref. 16)].

At CERN collider energies, the production of weak bosons is due mostly to valence quarks, as we show in Fig. 1. If Eqs. (18) and (19) are used to extract d_V/u_V , the error on R_σ is rather small,³ only $\pm 2.0\%$. At the Tevatron, sea quarks play a more prominent role as shown in Fig. 1. Our ability to calculate R_σ is improved since more of the flux is due to sea quarks, for which $\bar{u} = \bar{d}$. In the extreme case that the cross sections are entirely due to sea quarks, and if $\bar{u} = \bar{d} = \bar{s}$, the ratio of flux factors is determined entirely by $\sin^2\theta_w$.

The data on F_2^n/F_2^p are at small Q^2 , whereas we would like to use them at $Q^2 = M_W^2$. However, despite the large Q^2 dependence of the individual structure functions in the small- x region, the evolution of the ratio F_2^n/F_2^p with Q^2 is observed to be small, as shown in Fig. 6. This is as expected from QCD.

The x region of the structure functions relevant to the weak-boson cross-section calculation at Tevatron ener-

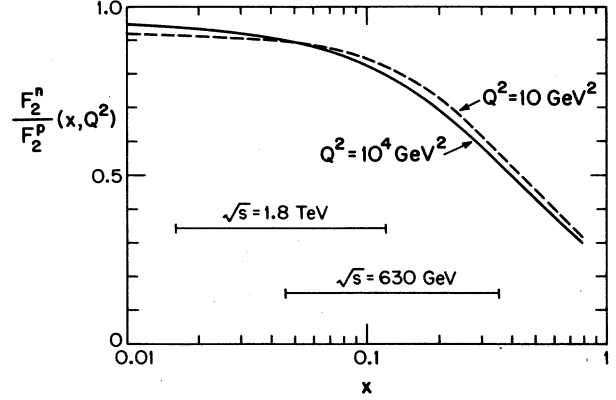


FIG. 6. The evolution of $F_2^n/F_2^p(x, Q^2)$ from $Q^2 = 10 \text{ GeV}^2$ to 10^4 GeV^2 as a function of x based on the MRS 1 parton densities (Ref. 11).

gies is unfortunately covered by only two deep-inelastic scattering experiments. In the CERN energy range seven experiments can be averaged⁷ for the calculation of the W -to- Z cross-section ratio. With only the BCDMS and EMC experiments providing input data at Tevatron energies, one not only loses statistics but also has to allow for systematic errors which could be common to both experiments. In order to extract d_V from F_2^n/F_2^p we interpolate the data points linearly and use Eq. (18) or (19) along with input values for u_V and the sea distributions for four choices of parton densities.^{9-11,16} Our final result $R_\sigma(\text{avg})$ is obtained by averaging the four calculations. The error is obtained by a similar procedure. We now interpolate the top (bottom) of the error bar of input data point i , including the full systematic error, with the middle of the adjacent data points and evaluate $R_\sigma(i)$ and

$$\Delta R_\sigma(i) = R_\sigma(i) - R_\sigma(\text{avg}). \quad (20)$$

This is repeated for each data point i . The errors $\Delta R_\sigma(i)$ are next weighted according to the magnitude of their relative contribution $\mathcal{W}(i)$ to the W -to- Z cross-section ratio. The final error is defined to be

$$\Delta R_\sigma = \sum_i \Delta R_\sigma(i) \mathcal{W}(i). \quad (21)$$

This procedure yields the following results:

$$R_\sigma = 3.08 \pm 0.05 \quad (\text{from BCDMS}) \\ = 3.11 \pm 0.06 \quad (\text{from EMC}) \quad (22)$$

and, after the two determinations are averaged,

$$R_\sigma = 3.10 \pm 0.04. \quad (23)$$

In Eq. (23) the error does not include experimental errors on M_W , $\sin^2\theta_w$, and Λ_{QCD} . After the change in R_σ is computed for 1σ variations of each of these quantities, the total error is obtained by adding individual contributions to the error in quadrature. The final result is

$$R_\sigma = 3.10 \pm 0.06 \quad (\sqrt{s} = 1.8 \text{ TeV}). \quad (24)$$

This prediction does not include the contribution from the charm-quark density in the proton. This contribution, discussed in Sec. IV, raises R_σ to 3.24 ± 0.06 . Following the same procedure, including five other deep-inelastic scattering experiments covering the larger x range relevant to computations at $\sqrt{s} = 630$ GeV, we obtain

$$R_\sigma = 3.39 \pm 0.05 \quad (\sqrt{s} = 630 \text{ GeV}). \quad (25)$$

This value is compatible with our previous result⁷ in which systematic errors were neglected and an earlier version of the BCDMS data was used (with the new version of the BCDMS data, $R_\sigma = 3.33 \pm 0.03$) along with the six other sets of experimental data.

Another method may be employed to calculate R_σ . It gives a value very close to our Eq. (23) and therefore adds to our confidence in it. It is based on the observation that published parton densities yield curves which bracket the EMC and BCDMS data on F_2^n/F_2^p ; the Duke-Owens⁹ set does so from above and the Eichten, Hinchliffe, Lane and Quigg¹⁰ set from below. This point is illustrated in Fig. 2. Using these parton densities, we compute $R_\sigma = 3.09$ (DO 1) and $R_\sigma = 3.144$ (EHLQ 1) at $\sqrt{s} = 1.8$ TeV (without inclusion of charm). The average of these is

$$R_\sigma = 3.12 \pm 0.03, \quad (26)$$

entirely consistent with our Eq. (23).

In Fig. 7, we show the standard-model prediction of the ratio R of $W \rightarrow e\nu$ and $Z \rightarrow e^+e^-$ events at the Tevatron for $N_\nu = 3, 4,$ and 5 light neutrino flavors, as a function of the top-quark mass. The rise in R above $m_t \approx M_Z/2$ results because the decay $Z \rightarrow t\bar{t}$ is no longer allowed while $W \rightarrow t\bar{b}$ is still kinematically allowed. When $m_t > M_W - m_b$ both decays are forbidden and R becomes independent of m_t . The limit on $N_\nu = 4$ can be weakened³ by addition of a heavy charged lepton, as the decay channel $W \rightarrow \nu L_4$ reduces the value of R by about

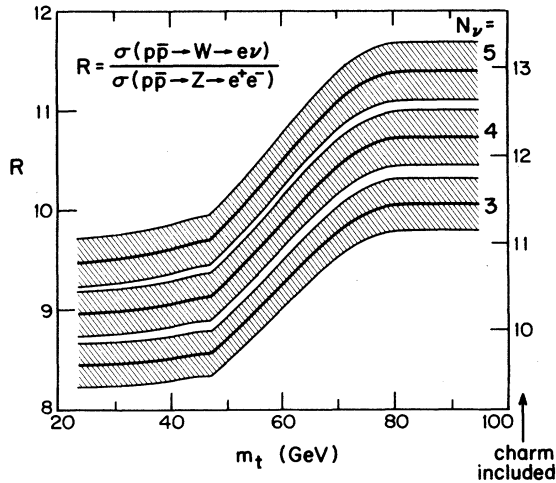


FIG. 7. The prediction of the ratio R of $W \rightarrow e\nu$ to $Z \rightarrow e^+e^-$ events at $\sqrt{s} = 1.8$ TeV is plotted as a function of m_t , for $N_\nu = 3, 4,$ and 5 , with (right-hand scale) and without (left-hand scale) inclusion of contributions from the charm quark.

0.5 for $M_L = 41$ GeV, which is the present UA1 lower limit.

Given an experimental upper limit on R and a choice of N_ν , the lower edge of each of the shaded bands in Fig. 7 will provide an upper bound on the mass of the top quark. The curves also permit various conclusions concerning the number of light neutrinos. First, a measured value of R less than about 8.2 would be inconsistent with the standard model. Second, a value greater than about 10.3 would require more than three light neutrino flavors. Finally, values between 8.2 and 10.3 would accommodate three, four, or five light neutrinos depending on m_t .

IV. CHARM-QUARK CONTRIBUTION TO WEAK-BOSON PRODUCTION

Thus far in our discussion we have ignored the presence of the charm-quark sea in the proton and antiproton. It will contribute to weak-boson production via $c\bar{s} \rightarrow W^+$ and $c\bar{c} \rightarrow Z$. Unfortunately, little is known experimentally about the charm-quark sea. We must therefore now rely on theoretical estimates, but we will show how high luminosity $p\bar{p}$ data can be used to measure the charm content of the proton in the near future.

The distribution function of a heavy quark Q is calculable perturbatively, provided $m_Q \gg \Lambda_{\text{QCD}}$. It is uncertain whether the charm quark is sufficiently heavy to allow a perturbative calculation. Nevertheless, charm-quark distribution functions have been calculated^{10,17} and we can use them to give some indication of the size of the contribution of the charm-quark sea to weak-boson production.

The charm-quark sea arises perturbatively from the splitting of gluons into $c\bar{c}$ pairs. Therefore, the process $c\bar{s} \rightarrow W^+$ will be accompanied by a spectator \bar{c} in the beam jet. If the W boson and the \bar{c} decay leptonically, the final state will contain opposite-sign leptons plus missing energy. The process $c\bar{c} \rightarrow Z$ will be accompanied by a spectator c and \bar{c} , and may thus give rise to up to four charged leptons.

In Fig. 8 we show the total cross section for W - and Z -

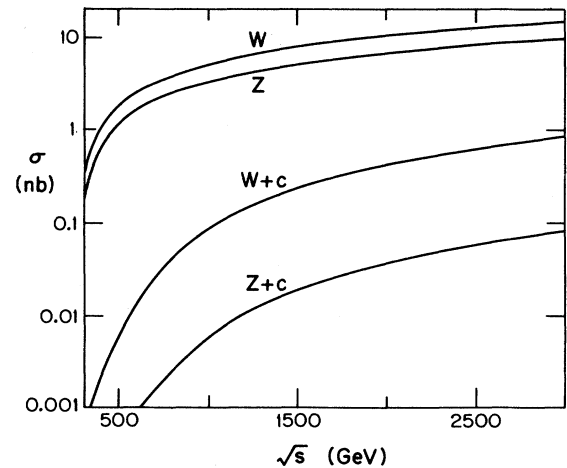


FIG. 8. The charm-quark contribution to W and Z production as a function of \sqrt{s} compared with the contributions from $u, d,$ and s . The EHLQ 1 parton densities are used.

boson production from charm quarks as a function of the total hadronic energy separately from the contribution from u , d , and s quarks. The charm-quark sea is clearly more significant for W -boson production than for Z -boson production. Although it contributes only about 1% of the total W -boson cross section at $\sqrt{s} = 630$ GeV, it contributes about 4% at the Tevatron energy $\sqrt{s} = 1.8$ TeV. Including the charm-quark contribution we find that the ratio of $\sigma(W)/\sigma(Z)$ quoted in the previous section is raised to 3.24 ± 0.06 from 3.10 ± 0.06 at $\sqrt{s} = 1.8$ TeV. In this sense our lack of knowledge of the charm-quark sea may be a large source of error in the calculation of $\sigma(W)/\sigma(Z)$.

It is difficult to assess the uncertainty in our knowledge of the charm-quark sea. Fortunately, its presence always increases $\sigma(W)/\sigma(Z)$, thereby tightening the limits on m_t and N_ν quoted in the previous section. Explicit results are shown in Fig. 7. Our neglect of the charm-quark sea in Sec. III would lead therefore to conservative conclusions on m_t . Experiments suggest that the charm-quark sea is less than half of the strange-quark sea.¹⁸ This constraint is satisfied by the charm-quark sea distribution we used.

The presence of a spectator \bar{c} accompanying $c\bar{s} \rightarrow W^+$ could perhaps be used as a tag to indicate W -boson production from the charm. This would in turn provide a measurement of the charm-quark sea. This would serve both to check the theoretical calculation of the charm-quark sea and to quantify the error in our knowledge of it.

Finally, let us comment on the process $g\bar{s} \rightarrow W^+\bar{c}$, depicted in Fig. 9, which also produces W bosons in association with \bar{c} . Although it is formally $O(\alpha_s)$ with respect to $c\bar{s} \rightarrow W^+$, the charm-quark sea itself is $O(\alpha_s)$, since it is generated perturbatively from gluons splitting into $c\bar{c}$. One is thus tempted to include both processes in a complete calculation of W -boson production. However, the process $c\bar{s} \rightarrow W^+$ is actually contained in the process $g\bar{s} \rightarrow W^+\bar{c}$. This point can be appreciated if the first diagram in Fig. 9 is examined in the limit that the t -channel charm quark is collinear with the incident gluon. Inclusion of both processes would thus constitute double counting.

A consistent formalism which avoids double counting is available. The $c\bar{s} \rightarrow W^+$ subprocess is subtracted from $g\bar{s} \rightarrow W^+\bar{c}$, and then added back via a charm-quark distribution function.¹⁹ The advantage of this method over the simple use of $g\bar{s} \rightarrow W^+\bar{c}$ is that the charm-quark distribution function includes the effects of gluon radiation

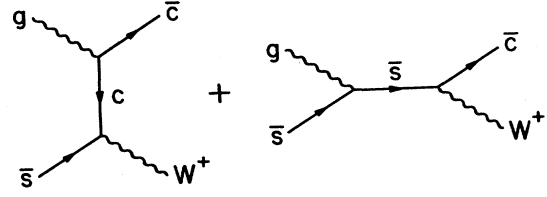


FIG. 9. Feynman diagrams for the associated production of W^+ with charm, which are formally $O(\alpha_s)$ with respect to $c\bar{s} \rightarrow W^+$. However, inclusion of both processes would constitute double counting.

to all orders in α_s in the leading-log approximation. The result is thus a renormalization-group-improved calculation of W -boson production in association with charm.

The prescription for subtracting $c\bar{s} \rightarrow W^+$ from $g\bar{s} \rightarrow W^+\bar{c}$ depends on the definition of the charm-quark distribution function. We have used the $\overline{\text{MS}}$ (modified minimal-subtraction scheme) distribution function of Ref. 17, for which the prescription is to regulate dimensionally the t -channel pole in $g\bar{s} \rightarrow W^+\bar{c}$ (with neglect of the charm-quark mass) and to simply discard the infinite part as in $\overline{\text{MS}}$ renormalization. A simple calculation²⁰ for the subtracted process $g\bar{s} \rightarrow W^+\bar{c}$ yields

$$\hat{\sigma} = \frac{\pi}{12} \alpha_s(\mu^2) \frac{\alpha}{\sin^2 \theta_W} \frac{1}{\hat{s}} \left[[\tau^2 + (1-\tau)^2] \ln \left[\frac{(1-\tau)^2}{\tau} \frac{M_W^2}{\mu^2} \right] + \frac{3}{2} + \tau - \frac{3}{2} \tau^2 \right], \quad (27)$$

where $\tau = M_W^2/\hat{s}$ and μ^2 is $O(M_W^2)$. We have neglected terms of order m_c^2/M_W^2 in this calculation.

Numerically, this subtracted cross section is not significant—it amounts to a 15% decrease in the cross section from $c\bar{s} \rightarrow W^+$. Thus the naive calculation of $c\bar{s} \rightarrow W^+$ is a good approximation to W -boson production from charm. Furthermore, this correction should *not* be included in a calculation of $\sigma(W)/\sigma(Z)$. It applies to all $q\bar{q} \rightarrow W, Z$ processes and therefore cancels in the ratio.

ACKNOWLEDGMENTS

This research was supported in part by the University of Wisconsin Research Committee with funds granted by the Wisconsin Alumni Research Foundation, and in part by the U.S. Department of Energy under Contracts Nos. DE-AC02-76ER00881 and W-31-109-ENG-38.

¹F. Halzen and M. Mursula, Phys. Rev. Lett. **51**, 857 (1983).

²A. Datta *et al.*, Phys. Rev. D **37**, 1876 (1988).

³F. Halzen, C. S. Kim, and S. Willenbrock, Phys. Rev. D **37**, 229 (1988).

⁴A. D. Martin, R. G. Roberts, and W. J. Stirling, Phys. Lett. B **189**, 220 (1987); Report No. DTP/88/12, 1988 (unpublished); P. Colas, D. Denegri, and C. Stubenrauch, Z. Phys. C **40**, 527 (1988).

⁵J.-J. Aubert *et al.*, European Muon Collaboration Nucl. Phys.

B293, 740 (1987).

⁶A. Milsztajn, Bologna-CERN-Dubna-Munich-Saclay Collaboration Ph.D. thesis, Université Paris XI.

⁷J. R. Cudell, F. Halzen, and C. S. Kim, Int. J. Mod. Phys. A **5**, 1051 (1988).

⁸J. Kubar, M. Le Bellac, J. L. Meunier, and G. Plaut, Nucl. Phys. **B175**, 251 (1980); G. Altarelli, R. K. Ellis, M. Greco, and G. Martinelli, *ibid.* **B246**, 12 (1984).

⁹D. Duke and J. Owens (DO), Phys. Rev. D **30**, 49 (1984).

- ¹⁰E. Eichten, I. Hinchliffe, K. Lane, and C. Quigg (EHLQ), *Rev. Mod. Phys.* **56**, 579 (1984).
- ¹¹A. D. Martin, R. G. Roberts, and W. J. Stirling (MRS), *Phys. Rev. D* **37**, 1161 (1988).
- ¹²An analysis of CERN UA1 data on W production to extract information on quark densities is presented in G. Arnison *et al.*, *Lett. Nuovo Cimento* **44**, 1 (1985).
- ¹³T. H. Chang, K. J. F. Gaemers, and W. L. Van Neerven, *Nucl. Phys.* **B202**, 407 (1982); V. Barger and R. J. N. Phillips, *Collider Physics* (Addison-Wesley, Reading, MA, 1987).
- ¹⁴K. Hikasa, *Phys. Rev. D* **29**, 1939 (1984).
- ¹⁵D. Dicus and S. Willenbrock, *Phys. Rev. D* **34**, 148 (1986).
- ¹⁶M. Glück, E. Hoffmann, and E. Reya (GHR), *Z. Phys. C* **13**, 119 (1982); J. F. Owens and E. Reya (OR), *Phys. Rev. D* **17**, 3003 (1978).
- ¹⁷J. C. Collins and W.-K. Tung, *Nucl. Phys.* **B278**, 934 (1986).
- ¹⁸H. Abramowicz *et al.*, *Z. Phys. C* **13**, 199 (1982); **17**, 283 (1983).
- ¹⁹R. M. Barnett, H. E. Haber, and D. Soper, *Nucl. Phys.* **B306**, 697 (1988); F. Halzen and C. S. Kim, *Int. J. Mod. Phys. A* **2**, 1069 (1987); F. Olness and W.-K. Tung, *ibid.* **2**, 1413 (1987).
- ²⁰G. Altarelli, R. K. Ellis, and G. Martinelli, *Nucl. Phys.* **B157**, 461 (1979).